

Design, Molecular Docking, Synthesis, Characterization and Preliminary Evaluation of Novel 1,3,4-Oxadiazole Derivatives as Cyclin-Dependent Kinase 2 Inhibitors

Yousef Sabah Ali*, Monther Faisal Mahdi*, Basma Monjid Abd Razik*, Talal Aburjai**

*Department of Pharmaceutical Chemistry, College of Pharmacy, Mustansiriyah University, Baghdad, Iraq.

**The University of Jordan, School of Pharmacy, Department of Pharmaceutical Sciences. Amman, Jordan.

Article Info:

Received Dec 2023

Revised Feb 2024

Accepted Mar 2024

Published Jan 2025

Corresponding Author email:

yousefsabah93@uomustansiriyah.edu.iq

Orcid: <https://orcid.org/0000-0002-8929-5786>

DOI: <https://doi.org/10.32947/ajps.v25i1.1132>

Abstract:

Novel 1,3,4-oxadiazole derivatives were designed, synthesized by reaction of semicarbazide hydrochloride with thiophene-2-carbaldehyde to form semicarbazone that undergo iodine-mediated cyclization to form 5-(thiophen-2-yl)-1,3,4-oxadiazol-2-amine which further reacted with different aldehydes to form Schiff base derivatives, and *in-vitro* tested for their cytotoxic activity. In a molecular docking study,

these chemicals were docked with the crystal structure of the cyclin-dependent kinase 2 protein (PDB code 2R3J) to assess their binding affinity. The recently developed analogues were validated, confirmed, and characterized using spectroscopic elemental analysis (FT-IR, ¹H-NMR, and ¹³C-NMR). Furthermore, these compounds underwent physicochemical, drug-like, and toxicological predictions. The molecular docking investigation shows that 1,3,4-oxadiazole derivatives bind strongly to the CDK-2 protein's active binding site. From the studied molecules, compounds 5a and 5d had the highest binding, with docking scores of -10.654 and -10.169 kcal/mol. The reference ligand binding score was -9.919 kcal/mol. As assessed by their anti-proliferative effects, compounds 5a and 5d showed promising cytotoxicity against colon cancer in Caco-2 cells. The compounds had IC₅₀ values of 43.16 and 60.8 μM at 24 hours, respectively, compared to the standard flavopiridol (59.2 μM). The findings of the cytotoxicity investigation and molecular docking analysis of these final derivatives (5a-5g) demonstrated a strong correlation, indicating the importance of a comprehensive pharmacological study to comprehend the anti-cancer mechanisms of these newly synthesized compounds fully.

KEYWORDS: 1,3,4-Oxadiazole, Colon Cancer, Molecular Docking, Schiff's Bases.

تصميم، تحضير، وتقييم مشتقات جديدة من 1,3,4-اوksاديازول باستخدام الارساء الجزيئي كعوامل محتملة مضادة لسرطان القولون

يوسف صباح علي, منذر فيصل مهدي*, بسمة منجد عبد الرزاق**, طلال ابو رجيح
*فرع الكيمياء الصيدلانية، كلية الصيدلة، الجامعة المستنصرية، بغداد، العراق.
**الجامعة الاردنية، كلية الصيدلة، قسم العلوم الصيدلانية، عمان، الاردن.



الخلاصة:

تم تصميم، تصنيع وتشخيص مشتقات جديدة لحلقة 1,3,4-او كساديازول الجديدة واختبارها داخل المختبر للتأكد من نشاطها السام للخلايا. في دراسة الارساء الجزيئي، تم ربط هذه المواد الكيميائية بالبنية البلورية لبروتين CDK-2 (2R3J-PDB) لتقييم درجة الارتباط. باستخدام الخصائص الفيزيائية والكيميائية، طيف الاشعة تحت الحمراء الدقيق، طيف الرنين النووي المغناطيسي للبروتون، وطيف الرنين النووي المغناطيسي للكربون، تم توصيف وتشخيص المركبات المصنعة. اشارت نتائج تحليل الارساء الجزيئي إلى أن مشتقات 1,3,4-او كساديازول اظهرت ارتباطاً قوياً داخل موقع الارتباط النشط لبروتين CDK-2. من بين الجزيئات التي تم اختبارها، أظهرت المركبات 5a و d5 أعلى درجة ارتباط 10.654- و 10.169- Kcal/mol على التوالي، بينما اظهرت الجزيئة المرجعية درجة ارتباط 9.919- Kcal/mol. أظهرت المركبات 5a و 5d نشاطاً بارزاً ومشجعاً مضاداً لسرطان القولون في خط خلايا Caco-2، أظهرت هذه المركبات قيم IC₅₀ تبلغ 43.16 و 60.8 ميكرومولار عند 24 ساعة، على التوالي، مقارنة بقيمة IC₅₀ لعقار فلأوبيريديول (59.2 ميكرومولار عند 24 ساعة). كانت نتائج تجارب السمية الخلوية التي أجريت على المركبات النهائية متوافقة مع نتائج بحث الارساء الجزيئي مما يشير إلى أهمية اجراء دراسة دوائية شاملة لفهم الآليات المضادة للسرطان لهذه المشتقات بشكل كامل.

الكلمات المفتاحية: 1,3,4-او كساديازول، الارساء الجزيئي، سرطان القولون، قواعد شف

1-Introduction

Cancer is a group of diseases characterized by uncontrolled cell growth and metastasis, the major cause of cancer mortality.⁽¹⁾ Globally, cancer is a major health concern, without effective therapies, cancer-related deaths will rise to 13 million in 2030 and 16 million in 2040.⁽²⁾ Despite the allocation of substantial personnel and material resources, a safe and efficacious agent for the treatment of cancer has yet to be developed. The clinical use of traditional cancer chemotherapeutic medicines is often linked with pervasive toxicity. Consequently, despite advancements in our comprehension of the biochemical pathways underlying carcinogenesis, the successful treatment of cancer continues to pose a significant challenge.⁽³⁾

Between a million and two million new cases of colorectal cancer (CRC) are reported yearly, making it the third most frequent malignancy and the fourth leading cause of cancer-related mortality globally. CRC ranks second among female cancer diagnoses (9.2%) and third among male diagnoses (10%).⁽⁴⁾ The genesis of colorectal cancer, like other cancers, can be attributed to mutations in certain genes. Oncogenes, tumor

suppressor genes, and DNA repair genes are susceptible to mutations.⁽⁵⁾

Interphase, the longest phase of the eukaryotic cell cycle, includes three subphases: G1 (where cells decide to grow or enter a quiescent state, G0), S phase (where DNA is produced), and G2 (where cells prepare for mitosis).⁽⁶⁾ Cyclin-dependent kinases (CDKs) regulate the initiation and progression of the cell cycle. The activity of several CDK genes in tumor cells is aberrant, with a specific significance in phosphorylating crucial elements in cell cycle.⁽⁷⁾ CDK-2 regulates the cycle by Cyclin A or E subunits phosphorylation. In G1 phase, CDK-4 and CDK-6 form complexes with D-type cyclin, which activates CDK-2 by interacting with cyclin E. In S phase, cyclin A binds CDK-2. After that, CDK-1 binds cyclin B in G2/M. Cyclin E activates CDK-2 to move the cell cycle from G1 to S phase, making it a main target for most anti-proliferative treatments.^(8,9)

Research on CDK inhibitors dates back to the 1990s. Pan-CDK inhibitors like Flavopiridol, Roscovitine, etc., represent the first generation of CDK inhibitors.⁽¹⁰⁾ Lack of selectivity and significant toxicity make the first generation of pan-CDK inhibitors harmful to normal cells. Recently discovered second-generation CDK inhibitors including



dinaciclib, P276-00, AT7519, TG02, roniciclib, RGB-286638, and others are more selective and less risky.^(11,12)

Cancer therapy has focused on heterocyclic chemicals, which include the active ring 1,3,4-oxadiazole and have intriguing cytotoxic potential. Oxadiazole is a five-member heterocyclic ring with two nitrogen atoms and one oxygen. Multiple isomers of oxadiazole exist.⁽¹³⁾ 1,3,4-oxadiazole derivatives are valuable because their active moiety affects their physicochemical and pharmacokinetic characteristics. 1,3,4-oxadiazole increased metabolic stability, hydrophilicity, and decreased lipophilicity. The 1,3,4-oxadiazole ring can serve as a bio-isostere for carbonyl, amide, ester, and carbamate molecules and constitute a substantial portion of the main ligand-interacting pharmacophore. As a flat aromatic moiety, it positions the molecule appropriately.^(14,15)

Compounds composing the 1,3,4-oxadiazole core exhibit potential of different

pharmacological activities such as antimicrobial^(16,17), anticancer^(18,19), antioxidant⁽²⁰⁾, anticonvulsant⁽²¹⁾, and anti-inflammatory.^(22,23)

The objective of this study was to employ a strategy involving the integration of a heterocyclic five-membered ring system, 1,3,4 oxadiazole, to synthesize novel derivatives. These derivatives were then assessed for their anti-proliferative activity against the human colon cancer Caco-2 and human dermal fibroblasts HdFn cell lines using the MTT method. The primary focus was to investigate the binding mode of these derivatives to CDK-2 and their potential impact on cancer cells.

2-Materials and methods

2.1 Chemicals and instruments

Table (1) shows the chemicals and instruments used during synthesis and characterization of intermediates and final molecules.

Table (1): Chemicals and instruments

Chemical	Company	Origin
1,4-dioxane	Alpha Chemika	India
2,3,4-trihydroxybenzaldehyde	Macklin	China
2-formylbenzoic acid	Macklin	China
2-phenylindole-3-carboxaldehyde	Macklin	China
Anhydrous sodium sulfate	Thomas Baker	India
Dichloromethane	Central Drug House CDH	India
Ethanol	Honeywell	Germany
Ethanol 99.9%	Scharlau	Spain
Glacial acetic acid	Thomas Baker	India
Helicin	Macklin	China
Indole-3-carboxaldehyde	Macklin	China
Iodine	Thomas Baker	India
Isoquinoline-5-carboxaldehyde	Macklin	China
Methanol	Loba Chemie	India
Potassium carbonate	Thomas Baker	India
Pyridoxal-5-phosphate hydrate	Macklin	China
Semicarbazide	Thomas Baker	India



Sodium acetate	Thomas Baker	India
Sodium thiosulfate	Thomas Baker	India
Thiophene-2-carbaldehyde	Macklin	China
Instrument	Company	Origin
Electrical melting point	Stuart	England
FT-IR Spectrometer	Shimadzu 8400s	Japan
NMR	Varian	USA
Sensitive Balance	Kern	Germany

2.2 Computational methods

The utilization of computational techniques is experiencing rapid growth and playing a pivotal position in the field of drug discovery due to their capacity to minimize the expenditure of time, financial resources, and labor. Docking is a strategy that involves predicting the form and orientation of ligands inside the active site of the target. Docking studies are conducted to accurately model the structure and gain precise understanding of the activity of substances.⁽²⁴⁾

ChemDraw16.0 (ChemOffice, 2016) was used to obtain 3D conformations of final derivatives. Spartan 14.0 with Monte-Carlo supported an optimizations process of 1500 interactions. Glide, a Schrodinger software, was used for molecular drug design and docking evaluation on a Windows 7 workstation (Intel(R) Core (TM) i7 CPU 895 @ 3.4GHz, 32 GB RAM, 1TB HD). CDK-2 crystal structure was retrieved from PDB under code 2R3J with a resolution of 1.65 Å. The ProPrep program was used to minimize and optimize this protein's structure, and the Lig Preprogram was used to prepare the structure of ligands prior to the docking step by adding hydrogen atoms and identifying the appropriate orientation and ionization position to achieve the lowest energy configuration of all derivatives. The grid box is set to be calibrated at 1.20 Å with 0.27 partial atomic, this specific size enables the unrestricted rotation of each component of the compounds being tested, facilitating the

AJPS (2025)

identification of the optimal conformation with the most favorable binding free energy.⁽²⁵⁾

The evaluation of ADME was previously conducted utilizing a readily available tool known as the Swiss-ADME web tool. This tool generates a collection of predictive models for PK parameters, physicochemical properties, medicinal chemistry, and drug-likeness. These properties include lipophilicity, bioavailability, water solubility, and BOILED-Egg.⁽²⁶⁾

2.3 Chemical synthesis

The procedure used for the synthesis of the intermediate and final compounds is described in **scheme 1**.

- Synthesis of (E)-2-(thiophen-2-yl methylene) hydrazine-1-carboxamide (3)

Semicarbazide hydrochloride (2) (0.5mmol, 0.055g) was mixed with sodium acetate NaOAc (0.5mmol, 0.041g) in distilled water H₂O (1mL). Thiophene-2-carbaldehyde (1) (0.5mmol, 0.056g) was dissolved in 1 mL of absolute methanol in a separate beaker. Both solutions were then mixed and agitated at room temperature for 30 minutes. The precipitate was filtered, collected, recrystallized using methanol, and dried.⁽²⁷⁾

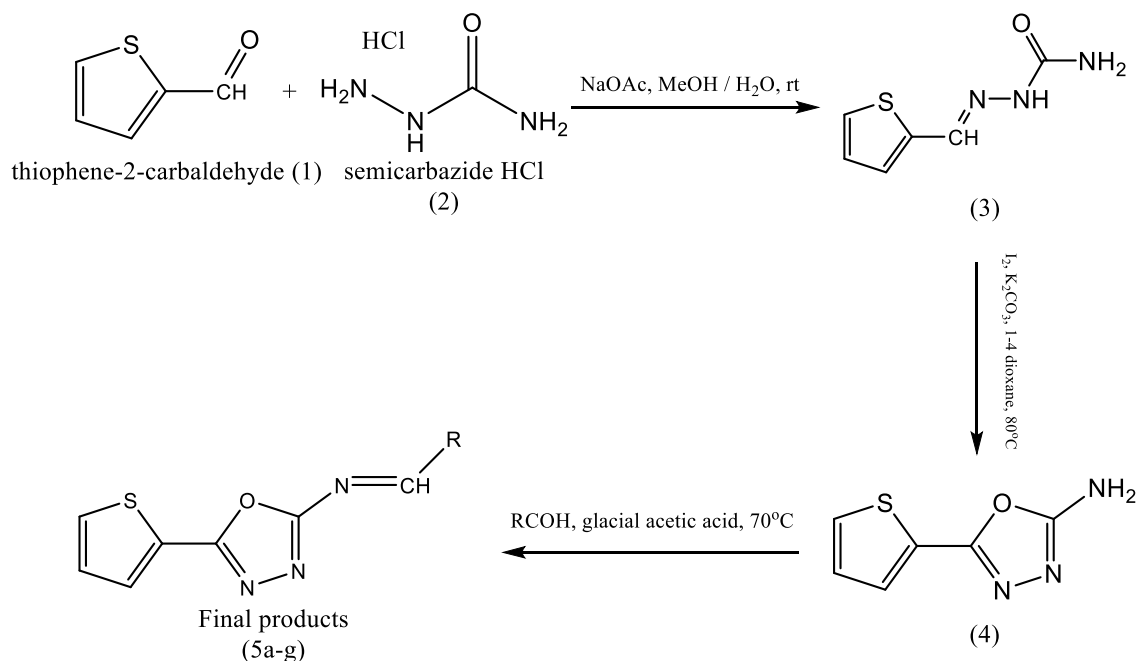


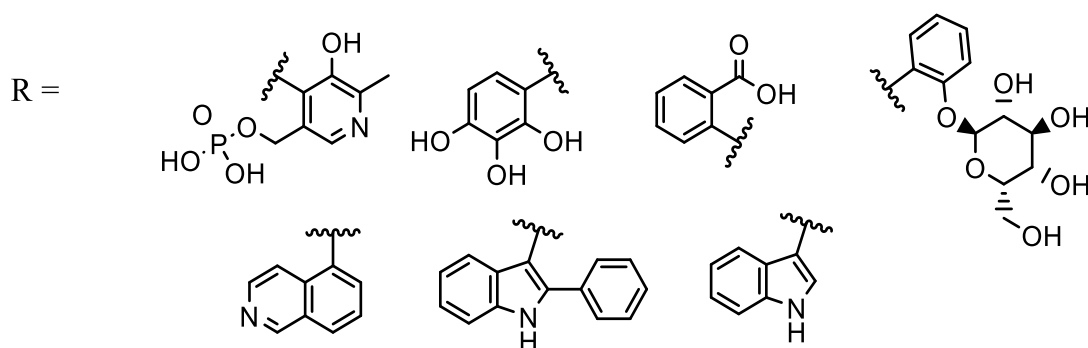
- **Synthesis of 5-(thiophen-2-yl)-1,3,4-oxadiazol-2-amine (4)**

After dissolving the residue (3) (0.5mmol, 0.084g) in 1,4-dioxane (5 mL), potassium carbonate (1.5mmol, 0.2g) and iodine (0.6mmol, 0.075g) were added successively. The reaction mixture was refluxed for 7 hours until complete. After cooling to room temperature, the substance was treated with 5% sodium thiosulfate $\text{Na}_2\text{S}_2\text{O}_3$ (20 mL) to remove excess iodine.⁽²⁸⁾ Extraction was performed using a 10:1 mixture of dichloromethane CH_2Cl_2 and methanol MeOH (10 mL \times 4). The organic layer was dried and concentrated with anhydrous sodium sulfate, and the residue was obtained.⁽²⁷⁾

- **General procedure for synthesis of Schiff base derivatives (5a-5g)**

Intermediate 4 (0.5mmol, 0.08g) was dissolved in 20 mL of absolute ethanol in a 100 mL round flask. The appropriate aromatic aldehydes were dissolved in 20 mL of absolute ethanol to make a 0.5 mmol solution in a separate flask, three to five drops of glacial acetic acid were progressively added to the solution of dissolved aldehydes. The aldehyde solution was slowly added to the intermediate solution after 15 minutes of continuous stirring. The mixture was then refluxed for 7 hours.^(29,30) After the reaction, the mixture was cooled to room temperature. It then evaporated, forming a solid precipitate. This precipitate was dried and recrystallized in ethanol.





Scheme (1): Synthesis of intermediates and final products

2.4 Cytotoxic activity study

The MTT colorimetric technique was used to evaluate the anticancer activity of the novel compounds (5a-5g) against Caco-2 and HdFn cell lines which were obtained and stored within the cell bank located at the Faculty of Medicine's Pharmacology Department of the University of Malaya, situated in Kuala Lumpur, Malaysia.

- Storing and resuscitating of cell line

The cells were cryopreserved in liquid nitrogen at -80°C for 24 hours. After thawing at 37°C , 10 mL of fresh media was added, and cells were centrifuged. For cultivation, the cells were moved to a 75 cm^2 flask and resuspended in 25 mL of fresh media.⁽³¹⁾

- Cell maintenance

Caco-2 and HdFn cells were grown in Roswell Park Memorial Institute (RPMI) media with 10% FBS and 1% penicillin-streptomycin-sodium bicarbonate as an antiseptic. The cells were cultivated in 75 mL flasks at 37°C , and 5% CO_2 . After 90% confluence, cell lines were aseptically transferred to other flasks. Following this, a trypsin solution was used to incubate cells on the flask surface for two minutes at 37°C to separate them. Additionally, the cells were centrifuged at 1200 RPM for three minutes.

After removing the liquid component holding the particles in suspension, the cells that had formed aggregates were reinserted into a fresh growth medium with added nutrients. Thus, cellular counts were determined using a hemocytometer under microscopic supervision and used as needed.⁽³²⁾

A 200 μl cell suspension of 5×10^4 - 5×10^6 cells was applied to each well of a 96-well flat-bottom tissue culture plate. For 24 hours, plates were incubated at 37°C , 5% CO_2 . The cells were treated with two-fold serial dilutions of chemicals (400, 200, 100, 50, and 25 μM). After cell culture, plates were incubated at 37°C , 5% CO_2 for 4 hours with triplicates of each concentration and control. Culture media was changed within 24 hours. After exposing the cells to a 10 μl MTT solution (5 mg/mL MTT powder dissolved in phosphate-buffered saline), they were incubated at 37°C , 5% CO_2 for 4 hours. After discarding the medium, 100 μl of dimethyl sulfoxide (DMSO) was added to each well. Incubate for 15-20 minutes at ambient temperature in darkness.⁽³³⁾

The optical density of each well was measured at 575 nm using an ELISA reader. Statistical examination of optical density data determined the chemical concentration needed to reduce cell viability by 50% for each cell line:



$$\text{Inhibition Rate percentage} = \frac{(A - B)}{A} * 100$$

Where A and B correspond to the optical density values of the standard compound and the compounds being tested, respectively.⁽³⁴⁾

- Determination of the half-maximal inhibitory concentration (IC₅₀)

To calculate the IC₅₀ of derivatives (5a-g), a dose-response curve was used. The "IC₅₀" of the *in-vitro* MTT procedure is the chemical concentration that causes a 50% reduction in cell viability.⁽³⁵⁾ The IC₅₀ values were calculated using compound concentrations of 400, 200, 100, 50, and 25 μM.

3-Results and discussion

3.1 Interpretation of docking results

From various crystallographic structures of CDK-2 stored in the protein data bank, the structure with the PDB code 2R3J was chosen. This specific structure was defined with an inhibitor that has bicyclic cores. The crystal structure of the ligand, 3-bromo-5-phenyl-N-(pyridin-3-ylmethyl) pyrazolo [1,5-a] pyrimidin-7-amine, is well-defined, showing its specific binding interactions with the CDK-2 protein.⁽³⁶⁾

The screening of the final compounds (5a-5g) resulted in binding scores spanning from (-10.654) to (-8.545) Kcal/mol on the 2R3J protein. In comparison, the reference ligand SCJ, which has already been crystallized with the receptor protein, had a score of (-9.916) Kcal/mol. From the results of table 1, compounds (5a) and (5d) showed the highest docking scores, -10.654 Kcal/mol, and -10.169 Kcal/mol respectively. This indicates their strong binding affinity and precise positioning within the active site of the target protein.

Table 2. illustrated the docking scores in Kcal/mole for each compound besides the number of hydrogen bonds, hydrophobic interactions with various amino acids, and pi-pi stacking interactions. **Figure 1.** exhibited a two-dimensional illustration of both highest scoring compounds 5a and 5d within the active binding site of CDK-2 protein.

3.2 Interpretation of ADME results

Utilizing *in silico* strategies to forecast the pharmacokinetic parameters of probable drug candidates in the lead generation and optimization steps has demonstrated an enhanced prospect of enduring the rapid turnover rates of drug discovery. To accelerate the process of discovering innovative drugs, there have been attempts to incorporate pharmacokinetic and developmental variables at an early stage of research. The aim is to select compounds that have a higher potential for binding optimization.

Table 3. illustrates the predicted parameters of drug-likeness and ADME for the designed products (5a-5g). Except for compounds (5a) and (5d), all molecules had TPSA values below 140 Å². All these compounds have bioavailability scores of 0.55 except compound (5a), which has 0.11 score. This disparity shows most compounds can enter the systemic circulation. Most compounds have significant gastrointestinal absorption following oral delivery. None of these compounds can cross the BBB. Except for compounds (5a) and (5f), none of the molecules bind to P-gp, a protein that prevents chemotherapeutic drugs from entering cells. These chemicals are not P-gp substrates; thus, efflux transporters cannot remove them from cells. All predicted molecules followed Lipinski's rule of five.



Table (2): Docking scores and interactions of final compounds (5a-5g) within CDK-2 active site

Compound	Docking score Kcal/mol	Hydrogen bonding	Hydrophobic interaction and Pi-Pi Stacking
5a	-10.654	ASP145, ILE10, GLU12 (2), THR14	LEU83 GLU81 PHE82 PHE80, VAL64 VAL18 ASP145 LEU148 TYR15 ILE10 THR14 GLY13 GLU12 GLY11
5b	-8.694	LEU83 (2)	ASP86 ALA31 GLN85 HIE84 LEU83 PHE82 LEU134 ASN132 GLU162 GLN131 GLU12 LYS129 GLY13 GLY11 ILE10
5c	-8.545	GLU81, LEU83	ASP86 GLU81 GLN85 ALA31 HIE84 LEU83 PHE82 PHE80 LYS33 ALA144 ILE10 ASP145 VAL18 LEU134 GLU8
5d	-10.169	ASP145 ASP86, ILE10, THR14	LYS33 HIE84 ALA31 PHE80 GLU81 LYS20 PHE82 LEU83 GLN85 ASP86 GLY11 VAL18 GLU8 ILE10 GLU12 GLY13 THR14
5e	-9.286	LEU83	VAL18 THR14 ILE10 GLY11 GLU12 GLY13 GLU162 VAL164 LYS129 PHE80 GLN131 ASN132 GLU81 PHE82 LEU83 LEU134
5f	-9.272	ASP145	ASP86 HIE84 LEU83 VAL64 PHE82 GLU81 GLN85 PHE80 ALA144 ASP145 LYS129 GLN131 LEU134 GLY13 GLU12 GLY11 ASN132 ILE10 GLU8. Pi-Pi stacking with PHE80
5g	-8.665	GLU81	GLU8 LYS20 VAL18 GLN85 LEU148 ASP145 ILE10 PHE80 GLU81 PHE82 LEU83 ALA144 HIE84 ASP86
SCJ	-9.916	LEU84, water molecule 1188	GLY14 GLY12 ILE11 GLU13 GLU9 PHE81 VAL19 ALA32 ALA145 ASP146 GLU82 HIS85 LEU84 ASP87 GLN86

Table (3): Output parameters of drug-likeness and ADME

Compound	nHBA ¹	nHBD ²	TPSA ³	Bioavailability	GI absorption	BBB penetration	P-gp ⁴	Lipinski Ro5 ⁵	M _w t
5a	10	3	189.21	0.11	Low	No	Yes	No violation	396.31
5b	7	3	140.21	0.55	High	No	No	No violation	303.29
5c	6	1	116.82	0.56	High	No	No	No violation	299.30
5d	10	4	178.90	0.55	Low	No	No	No violation	433.44
5e	5	0	92.41	0.55	High	No	No	No violation	306.34
5f	4	1	95.31	0.55	High	No	Yes	No violation	370.43
5g	4	1	95.31	0.55	High	No	No	No violation	294.33

¹ Number of hydrogen bond acceptors

² Number of hydrogen bond donors

³ Topological polar surface area

⁴ P-glycoprotein efflux

⁵ Lipinski rule of five



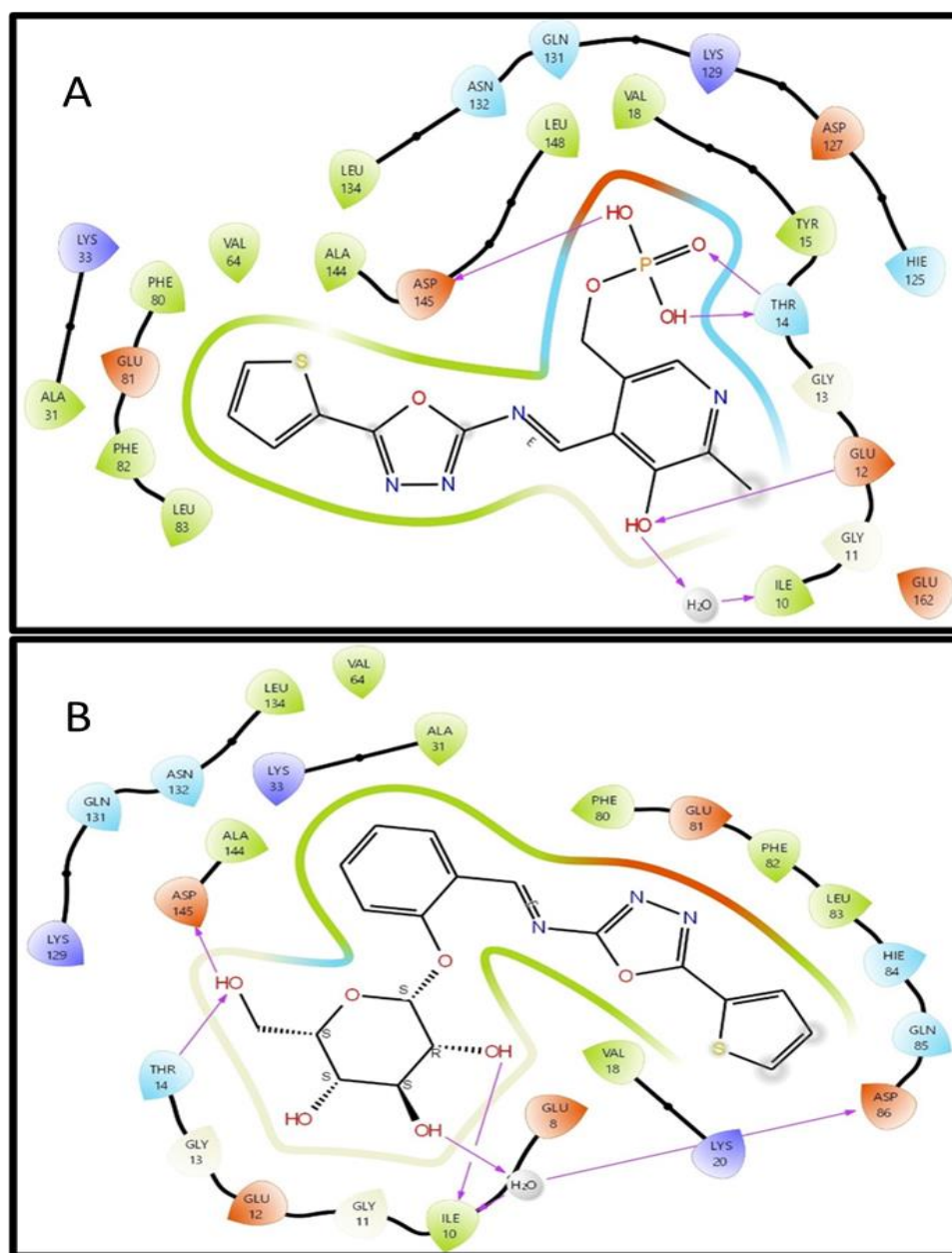


Figure (1): Two-dimensional illustration of (A) compound 5a and (B) compound 5d inside CDK-2 active site.

3.3 Interpretation of synthetic studies

Compound (3) was formed by initial protonation of thiophene-2-carbaldehyde in an acidic medium followed by nucleophilic attack from nitrogen atom of semicarbazide to form the carbinolamine intermediate, which undergoes dehydration ($-H_2O$) to produce the iminium ion. Finally, iminium

ion loses a proton from the nitrogen atom to produce the compound 3.⁽³⁷⁾ The chemical structure of compound (3) was determined using FT-IR. Results showed doublet bands at 3454 and 3279 for primary amine, and 3240 for secondary amide N-H, band at 2989 for imine group C-H bond, band at 1687 for carbonyl group C=O, and a characteristic

band at 1647 for C=N stretching vibration, indicating imine group formation.

Compound (4) was formed by oxidative iodination of compound (3) to generate an iodide intermediate which undergoes an S_N2 type of cyclization to generate another intermediate with the formation of new C-O bond. Finally, the subsequent deprotonation of the later intermediate by base leads to the formation of the oxadiazole ring.⁽³⁸⁾ The FT-IR spectra of compound (4) shows characteristic bands at 3259 for stretching vibration of amine group NH_2 , disappearance of the strong band at 3240 indicates the deprotonation of nitrogen atom of amide group and formation of C=N bond of the oxadiazole ring, the strong band at 1651 for stretching vibration of oxadiazole C=N bond, the disappearance of 2989 band and 1687 band indicates the removal of a proton from imine group and the removal of carbonyl group C=O while the band at 1265 indicates the formation of C-O bond and oxadiazole ring. The 1H -NMR spectrum of compound (4) showed characteristic singlet peak at 7.29 ppm for the two protons of amine group and three peaks at 7.2, 7.5 & 7.7 ppm (t,d,d) for the three protons of thiophene ring. The ^{13}C -NMR spectrum of compound (4) showed characteristic four peaks at (126.11, 127.71, 128.81 & 129.42 ppm) for the four carbon atoms of thiophene ring and two peaks at 154.21 & 163.83 ppm for the two carbon atoms of oxadiazole ring.

FT-IR charts of all novel derivatives (5a-5g) showed disappearance of bands that belong to amine group of the intermediate (compound 4) in addition to band returning to carbonyl of the aldehyde from all synthesized compounds and appearance of newly characterized bands at the range of (1635 – 1660 cm^{-1}) which indicate the formation of C=N of imine group and bands at range of (2922 – 2978 cm^{-1}) returning for

the C-H vibration of carbon atom of imine group. 1H -NMR spectra for all novel compounds (5a-5g) demonstrate the elimination of signals returning to amine protons of the intermediate (4) and signal which return to proton of the aldehyde (CHO) and emergence of fresh singlet signal returning to the proton of imine group (N=CH) at range of (8.3 – 9.8 ppm). ^{13}C -NMR spectra of the synthesized compounds (5a-5g) showed the disappearance of signal which return to carbonyl carbon of aldehyde and appearance of new characteristic signal returning to imine group carbon at range of (149.58-169.64 ppm).

Compound (3) 2-(thiophen-2-ylmethylene) hydrazine-1-carboxamide.

Red to brown powder. Yield= 81%. m.p.= 237-239 °C. FTIR ν (cm^{-1}): 3454-3279 (N-H₂), 3240 (N-H), 2989 (H-C=N), 3070 (H-Ar), 1687 (C=O), 1647 (C=N), 1599-1531 (Ar C=C).

Compound (4) 5-(thiophen-2-yl)-1,3,4-oxadiazol-2-amine.

White powder. Yield= 54%. m.p.= 243-244 °C. FTIR ν (cm^{-1}): 3259 (N-H₂), 3109 (H-Ar), 1651 (C=N), 1600-1508 (Ar C=C). 1H -NMR (DMSO-d₆, 400 MHz, ppm): 7.21 (t, 1H, thiophene H), 7.29 (s, 2H, NH₂), 7.51 (d, 1H, thiophene H), 7.77 (d, 1H, thiophene H). ^{13}C -NMR (DMSO-d₆, 100 MHz, ppm): 126.11-129.42 (4C, thiophene C), 154.21, 163.83 (2C, oxadiazole C).

Compound (5a) (E)-(5-hydroxy-6-methyl-4-(((5-(thiophen-2-yl)-1,3,4-oxadiazol-2-yl) imino)methyl)pyridin-3-yl)methyl dihydrogen phosphate.



Yellow powder. Yield= 71%. m.p.= 212-214 °C. FTIR ν (cm^{-1}): 3265-3192 (O-H), 3117 (H-Ar), 2941 (H-C=N), 1654 (C=N), 1602-1573 (Ar C=C). $^1\text{H-NMR}$ (DMSO- d_6 , 400 MHz, ppm): 2.44 (s, 3H, pyridine CH₃), 5.19 (s, 2H, CH₂), 6.07 (s, 1H, pyridine OH), 7.21 (t, 1H, thiophene H), 7.52 (d, 1H, thiophene H), 7.77 (d, 1H, thiophene H), 8.29 (s, 1H, pyridine H), 9.08 (s, 1H, imine H), 10.17 (s, 1H, P-OH), 10.41 (s, 1H, P-OH). $^{13}\text{C-NMR}$ (DMSO- d_6 , 100 MHz, ppm): 18.98 (1C, CH₃), 69.31 (1C, CH₂), 126.09-129.44 (4C, thiophene C), 128.50-138.19 (5C, pyridine C), 154.20 & 163.83 (2C, oxadiazole C), 161.78 (1C, imine C=N).

Compound (5b) (E)-4-(((5-(thiophen-2-yl)-1,3,4-oxadiazol-2-yl)imino)methyl)benzene-1,2,3-triol.

Dark orange powder. Yield= 77%. m.p.= 175-176 °C. FTIR ν (cm^{-1}): 3304,3275,3186 (O-H), 3086 (H-Ar), 2944 (H-C=N), 1652 (C=N), 1612-1581 (Ar C=C). $^1\text{H-NMR}$ (DMSO- d_6 , 400 MHz, ppm): 6.53 (d, 1H, Ar H), 7.14 (d, 1H, Ar H), 7.22 (t, 1H, thiophene H), 7.55 (d, 1H, thiophene H), 7.78 (d, 1H, thiophene H), 9.87 (s, 1H, imine H). $^{13}\text{C-NMR}$ (DMSO- d_6 , 100 MHz, ppm): 124.30-129.39 (4C, thiophene C), 108.87-153.87 (6C, phenyl C), 154.23 & 163.84 (2C, oxadiazole C), 169.64 (1C, imine C=N).

Compound (5c) (E)-2-(((5-(thiophen-2-yl)-1,3,4-oxadiazol-2-yl)imino)methyl)benzoic acid.

Light grey powder. Yield= 74%. m.p.= 194-196 °C. FTIR ν (cm^{-1}): 3255 (O-H), 3105 (H-Ar), 2974 (H-C=N), 1770 (C=O), 1651 (C=N), 1616-1577 (Ar C=C). $^1\text{H-NMR}$ (DMSO- d_6 , 400 MHz, ppm): 7.21 (t, 1H, thiophene H), 7.53 (d, 1H, thiophene H), 7.77 (d, 1H, thiophene H), 7.25 (d, 1H, Ar H), 7.79 (t, 1H, Ar H), 7.85 (t, 1H, Ar H),

8.21 (d, 1H, Ar H), 9.51 (s, 1H, imine H). $^{13}\text{C-NMR}$ (DMSO- d_6 , 100 MHz, ppm): 124.41-131.46 (4C, thiophene C), 126.78-145.58 (6C, benzyl C), 154.22 & 163.84 (2C, oxadiazole C), 168.71 (1C, imine C=N), 169.01 (1C, carboxylic C).

Compound (5d) (2S,3S,4S,5R,6S)-2-(hydroxymethyl)-6-(2-((E)-((5-(thiophen-2-yl)-1,3,4-oxadiazol-2-yl)imino)methyl)phenoxy)tetrahydro-2H-pyran-3,4,5-triol.

Off-white powder. Yield= 76%. m.p.= 229-231 °C. FTIR ν (cm^{-1}): 3460-3255 (O-H), 3120 (H-Ar), 2922 (H-C=N), 1660 (C=N), 1597-1581 (Ar C=C). $^1\text{H-NMR}$ (DMSO- d_6 , 400 MHz, ppm): 3.32 (d, 2H, CH₂), 3.21 (t, 1H, cyclic CH), 3.35 (t, 1H, cyclic CH), 3.44 (t, 1H, cyclic CH), 3.74 (t, 1H, cyclic CH), 4.65 (s, 1H, cyclic OH), 5.00 (s, 1H, cyclic OH), 5.13 (s, 1H, cyclic OH), 5.20 (s, 1H, cyclic OH), 5.56 (d, 1H, cyclic CH), 7.21 (t, 1H, thiophene H), 7.52 (d, 1H, thiophene H), 7.77 (d, 1H, thiophene H), 7.16 (d, 1H, aromatic CH), 7.33 (t, 1H, aromatic CH), 7.66 (t, 1H, aromatic CH), 7.72 (d, 1H, aromatic CH), 9.64 (s, 1H, imine H). $^{13}\text{C-NMR}$ (DMSO- d_6 , 100 MHz, ppm): 61.13 (1C, CH₂), 70.1-101.43 (5C, tetrahydropyran C), 116.87-136.69 (6C, benzyl C), 127.35-129.40 (4C, thiophene C), 154.22 & 163.83 (2C, oxadiazole C), 160.35 (1C, imine C=N).

Compound (5e) (Z)-1-(isoquinolin-5-yl)-N-(5-(thiophen-2-yl)-1,3,4-oxadiazol-2-yl)methanimine.

Light brown powder. Yield= 83%. m.p.= 140-142 °C. FTIR ν (cm^{-1}): 3116 (H-Ar), 2973 (H-C=N), 1658 (C=N), 1600-1573 (Ar C=C). $^1\text{H-NMR}$ (DMSO- d_6 , 400 MHz, ppm): 7.20 (t, 1H, thiophene H), 7.51 (d, 1H, thiophene H), 7.75 (d, 1H, thiophene H), 7.92 (t, 1H, isoquinoline H), 8.44 (d, 1H,



isoquinoline H), 8.49 (d, 1H, isoquinoline H), 8.70 (d, 1H, isoquinoline H), 8.89 (d, 1H, isoquinoline H), 9.46 (s, 1H, imine H), 10.42 (s, 1H, isoquinoline H). ¹³C-NMR (DMSO-d₆, 100 MHz, ppm): 126.12-132.77 (4C, thiophene C), 117.36-146.27 (9C, isoquinoline C), 154.21-163.84 (2C, oxadiazole C), 153.57 (1C, imine C=N).

Compound (5f) (E)-1-(2-phenyl-1H-indol-3-yl)-N-(5-(thiophen-2-yl)-1,3,4-oxadiazol-2-yl)methanimine.

Red powder. Yield= 72%. m.p.= 199-201 °C. FTIR ν (cm⁻¹): 3267 (N-H), 3101 (H-Ar), 2978 (H-C=N), 1658 (C=N), 1627-1577 (Ar C=C). ¹H-NMR (DMSO-d₆, 400 MHz, ppm): 7.51 (d, 2H, Ar H), 7.53 (t, 2H, Ar H), 7.80 (d, 1H, Ar H), 7.23 (d, 1H, indole H), 7.27 (t, 1H, indole H), 7.63 (t, 1H, indole H), 8.24 (d, 1H, indole H), 7.21 (t, 1H, thiophene H), 7.59 (d, 1H, thiophene H), 7.77 (d, 1H, thiophene H), 8.79 (s, 1H, imine H), 12.43 (s, 1H, indole NH). ¹³C-NMR (DMSO-d₆, 100 MHz, ppm): 126.12-130.37 (4C, thiophene C), 124.19-130.25 (6C, benzyl C), 112.50-136.38 (8C, indole C), 154.22-163-85 (2C, oxadiazole C), 149.58 (1C, imine C=N).

Compound (5g) (E)-1-(1H-indol-3-yl)-N-(5-(thiophen-2-yl)-1,3,4-oxadiazol-2-yl)methanimine.

Yellow powder. Yield= 76%. m.p.= 180-181 °C. FTIR ν (cm⁻¹): 3242 (N-H), 3109 (H-Ar), 2975 (H-C=N), 1635 (C=N), 1608-1573 (Ar C=C). ¹H-NMR (DMSO-d₆, 400 MHz, ppm): 7.21 (d, 1H, indole H), 7.23 (t, 1H, indole H), 7.53 (t, 1H, indole H), 7.77 (d, 1H, indole H), 7.27 (t, 1H, thiophene H), 7.56 (d, 1H, thiophene H), 7.78 (d, 1H, thiophene H),

8.14 (s, 1H, indole H), 8.32 (s, 1H, imine H), 12.20 (s, 1H, indole NH). ¹³C-NMR (DMSO-d₆, 100 MHz, ppm): 112.91-138.95 (8C, indole C), 126.14-129.36 (4C, thiophene C), 154.26 & 163.87 (2C, oxadiazole C), 163.87 (1C, imine C=N).

3.4 Interpretation of cytotoxic studies

The MTT assay was employed to ascertain the IC₅₀ values of the synthesized compounds. The IC₅₀ values were determined by subjecting the cells to synthesized compounds (5a-5g) for 24 hours. Compounds 5a and 5d showed promising cytotoxic activity, with IC₅₀ values of 43.16 μ M and 60.8 μ M for Caco-2, 105.2 μ M and 155.2 μ M for HdFn, respectively, compared to the reference flavopiridol (59.2 μ M and 151.6 μ M, respectively) at 24 hours. Compound 5a is more toxic to cancer and normal cell lines than flavopiridol, while compound 5d is similar. Final drug cytotoxicity tests confirmed molecular docking predictions.

Compounds 5b, 5e and 5g showed potential activity against cancer cell line Caco-2 with IC₅₀ values (83.17 μ M, 88.4 μ M and 82.4 μ M, respectively) at 24 hours, while compounds 5c and 5f had the lowest toxicity against cancer cell line Caco-2 (IC₅₀ values: 134.9 μ M and 140.5 μ M, respectively) and the safest profile against normal cell line HdFn (IC₅₀ values: 185.9 μ M and 151.9 μ M, respectively).

Figure 2. illustrates the IC₅₀ dose-response curves of all synthesized compounds and standard treatment flavopiridol.



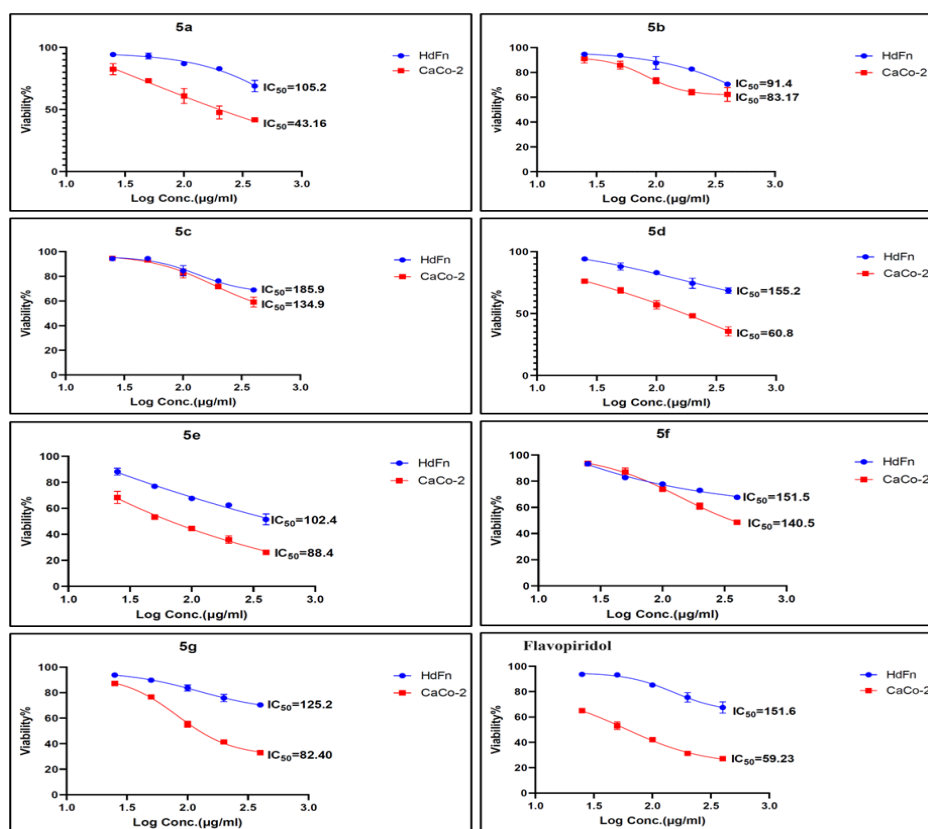


Figure (2): IC₅₀ dose response curve of synthesized compounds and flavopiridol after 24 hours.

4-Conclusions

A set of new 1,3,4-oxadiazole derivatives has been effectively designed, synthesized, identified, and assessed utilizing computational techniques, including ADME studies. The findings indicated that all compounds adhered to Lipinski's "rule of five", and were absorbed passively from the gastrointestinal system, apart from compounds 5a and 5d. The molecular docking analysis of the final compounds (5a-5g) demonstrated a substantial contact with the CDK-2 protein, with two derivatives (5a & 5d) exhibiting superior performance compared to the reference molecule SCJ. The synthesized compounds were assessed for their anti-proliferative potential against the CaCo-2 human colon cancer cell line and the HdFn human dermal fibroblasts cell line.

AJPS (2025)

Most produced compounds exhibited exceptional anti-proliferative action. The cytotoxicity and molecular docking investigations of the newly synthesized compounds (5a-5g) demonstrate a good and positive association.

References

- 1- Su Z, Yang Z, Xu Y, Chen Y, Yu Q. Apoptosis, autophagy, necroptosis, and cancer metastasis. *Mol Cancer*. February 2015. Vol.14(48).
- 2- Al-Anazi M, Khairuddean M, O. Al-Najjar B, Murwih Alidmat M, Nur Syazni Nik Mohamed Kamal N, Muhamad M. Synthesis, anticancer activity and docking studies of pyrazoline and pyrimidine derivatives as potential epidermal growth factor



- receptor (EGFR) inhibitors. Arab J Chem. July 2022. Vol.15(7).
- 3- Shawky AM, Abdalla AN, Ibrahim NA, Abourehab MAS, Gouda AM. Discovery of new pyrimidopyrrolizine/indolizine-based derivatives as P-glycoprotein inhibitors: Design, synthesis, cytotoxicity, and MDR reversal activities. Eur J Med Chem. June 2021. Vol.218.
 - 4- Katsaounou K, Nicolaou E, Vogazianos P, Brown C, Stavrou M, Teloni S, et al. Colon Cancer: From Epidemiology to Prevention. Metabolites. May 2022. Vol. 12(6). P: 499.
 - 5- Fearon ER, Vogelstein B. A genetic model for colorectal tumorigenesis. Cell. June 1990. Vol. 61(5). P: 759-67.
 - 6- Bai J, Li Y, Zhang G. Cell cycle regulation and anticancer drug discovery. Cancer Biol Med. November 2017. Vol. 14(4). P: 348-362.
 - 7- Chen J, Pang L, Wang W, Wang L, Zhang JZH, Zhu T. Decoding molecular mechanism of inhibitor bindings to CDK2 using molecular dynamics simulations and binding free energy calculations. J Biomol Struct Dyn. March 2020. Vol. 38(4) P: 985–96.
 - 8- Phoujdar MS, Aland GR. Molecular docking study on 1H-(3,4d) pyrazolopyrimidines as cyclin dependant kinase (CDK2) inhibitors. Int J Curr Pharm Res. December 2016. Vol. 9(1). P: 94.
 - 9- Peyressatre M, Prével C, Pellerano M, Morris MC. Targeting cyclin-dependent kinases in human cancers: from small molecules to Peptide inhibitors. Cancers. January 2015. Vol. 7(1). P: 179-237.
 - 10- Whittaker SR, Mallinger A, Workman P, Clarke PA. Inhibitors of cyclin-dependent kinases as cancer therapeutics. Pharmacol Ther. May 2017. Vol. 173. P: 83-105.
 - 11- Kargbo RB. Selective Cyclin-Dependent Kinase Inhibitors and Their Application in Cancer Therapy. ACS Med Chem Lett. October 2022. Vol. 13(10). P: 1561–3.
 - 12- Zhang M, Zhang L, Hei R, Li X, Cai H, Wu X, Zheng Q, Cai C. CDK inhibitors in cancer therapy, an overview of recent development. Am J Cancer Res. May 2021. Vol. 11(5). P: 1913-35.
 - 13- Housman G, Byler S, Heerboth S, Lapinska K, Longacre M, Snyder N, Sarkar S. Drug resistance in cancer: an overview. Cancers. September 2014. Vol. 6(3). P: 1769-92.
 - 14- Kavitha S, Gnanavel S, Kannan K. Biological aspects of 1,3,4-oxadiazole derivatives. Asian J Pharm Clin Res. August 2014. Vol. 7(4). P: 11-20.
 - 15- Boström J, Hogner A, Llinàs A, Wellner E, Plowright AT. Oxadiazoles in medicinal chemistry. J Med Chem. March 2012. Vol. 55(5). P: 1817–30.
 - 16- Chortani S, Edziri H, Manachou M, Al-Ghamdi YO, Almalki SG, Alqurashi YE, et al. Novel 1,3,4-oxadiazole linked benzopyrimidinones conjugates: Synthesis, DFT study and antimicrobial evaluation. J Mol Struct. October 2020. Vol. 1217.
 - 17- Jwaid MM, Ali KF, Abd-alwahab MH. Synthesis, Antibacterial study and ADME Evaluation of Novel Isonicotinoyl Hydrazide Derivative Containing 1,3,4-Oxadiazole Moiety. Al Mustansiriyah Journal of Pharmaceutical Sciences. December 2020. Vol. 20(4). P: 113-21.
 - 18- Bajaj S, Kumar MS, Tinwala H, YC M. Design, synthesis, modelling studies and biological evaluation of 1,3,4-oxadiazole derivatives as potent anticancer agents targeting thymidine phosphorylase enzyme. Bioorg Chem. June 2021. Vol. 111.



- 19- Alam MM, Almalki ASA, Neamatallah T, Ali NM, Malebari AM, Nazreen S. Synthesis of new 1, 3, 4-oxadiazole-incorporated 1, 2, 3-triazole moieties as potential anticancer agents targeting thymidylate synthase and their docking studies. *Pharmaceuticals*. November 2020. Vol. 13(11). P: 1–15.
- 20- Küçüköğlü K, Acar Çevik U, Nadaroglu H, Celik I, Işık A, Bostancı HE, et al. Design, synthesis and molecular docking studies of novel benzimidazole-1,3,4-oxadiazole hybrids for their carbonic anhydrase inhibitory and antioxidant effects. *Med Chem Res*. October 2022. Vol. 31(10). P: 1771–82.
- 21- Singh RB, Das N, Singh GK, Singh SK, Zaman K. Synthesis and pharmacological evaluation of 3-[5-(aryl-[1,3,4]oxadiazole-2-yl)]-piperidine derivatives as anticonvulsant and antidepressant agents. *Arab J Chem*. May 2020. Vol. 13(5). P: 5299–311.
- 22- Kashid BB, Salunkhe PH, Dongare BB, More KR, Khedkar VM, Ghanwat AA. Synthesis of novel of 2, 5-disubstituted 1, 3, 4-oxadiazole derivatives and their in vitro anti-inflammatory, anti-oxidant evaluation, and molecular docking study. *Bioorg Med Chem Lett*. June 2020. Vol. 30(12).
- 23- Kumar D, Kumar RR, Pathania S, Singh PK, Kalra S, Kumar B. Investigation of indole functionalized pyrazoles and oxadiazoles as anti-inflammatory agents: Synthesis, in-vivo, in-vitro and in-silico analysis. *Bioorg Chem*. September 2021. Vol. 114.
- 24- Omran SM, Abd Razik BM, Mahdi MF. Density functional theory and molecular modeling studies of new 4-(Furan-2-yl)thiazol-2-amine derivatives as cyclooxygenase inhibitors. *Egypt J Chem*. September 2021. Vol. 64(9). P: 4833–41.
- 25- Ali YS, Mahdi MF, Abd Razik BM. *In silico* evaluation of binding interaction and ADME properties of novel 5-(thiophen-2-yl)-1,3,4-oxadiazole-2-amine derivatives as anti-proliferative agents. *Int J App Pharm*. January 2023. Vol. 15(1). P: 141–6.
- 26- Daina A, Michielin O, Zoete V. SwissADME: A free web tool to evaluate pharmacokinetics, drug-likeness and medicinal chemistry friendliness of small molecules. *Sci Rep*. March 2017. Vol. 7.
- 27- Niu P, Kang J, Tian X, Song L, Liu H, Wu J, et al. Synthesis of 2-amino-1,3,4-oxadiazoles and 2-Amino-1,3,4-thiadiazoles via sequential condensation and I₂-mediated oxidative C-O/C-S bond formation. *J Org Chem*. January 2015. Vol. 80(2). P: 1018–24.
- 28- Nawghare BR, Gaikwad SV, Raheem A, Lokhande PD. Iodine catalyzed cascade synthesis of flavone derivatives from 2'-allyloxy- α,β -dibromo chalcones. *J Chil Chem Soc*. March 2014. Vol. 59(1). P: 291–302.
- 29- Jabbar ZA, Mahdi MF, Abd Razik BM. Synthesis, Characterization, ADME Study and Anti-proliferative evaluation against MCF-7 breast cancer cell line of new analog of a 4-aminophenyl quinazolinone derivative. *Al Mustansiriyah Journal of Pharmaceutical Sciences*. April 2023. Vol. 23(4). P: 411-28.
- 30- Mahdi MF, Raauf AMR, Kadhim FAH. Design, Synthesis and Acute Anti-Inflammatory Evaluation of New Non-Steroidal Anti-Inflammatory Agents Having 4-Thiazolidinone Pharmacophore. *J Nat Sci Res*. 2015. Vol. 5(6). P: 21-9.



- 31- Kaplan A, Akalin Ciftci G, Kutlu HM. The apoptotic and genomic studies on A549 cell line induced by silver nitrate. *Tumour Biol.* April 2017. Vol. 39(4). P: 1-12.
- 32- Shi Y, Tang B, Yu PW, Tang B, Hao YX, Lei X, Luo HX, Zeng DZ. Autophagy protects against oxaliplatin-induced cell death via ER stress and ROS in Caco-2 cells. *PLoS One.* November 2012. Vol. 7(11). P:1-8.
- 33- Chang J, Ren H, Zhao M, Chong Y, Zhao W, He Y, et al. Development of a series of novel 4-anilinoquinazoline derivatives possessing quinazoline skeleton: Design, synthesis, EGFR kinase inhibitory efficacy, and evaluation of anticancer activities in vitro. *Eur J Med Chem.* July 2017. Vol. 138. P: 669–88.
- 34- Shaaban OG, Abd El Razik HA, A Shams El-Dine SED, Ashour FA, El-Tombary AA, Afifi OS, et al. Purines and triazolo[4,3-e]purines containing pyrazole moiety as potential anticancer and antioxidant agents. *Future Med Chem.* June 2018. Vol. 10(12). P: 1449–64.
- 35- Sebaugh JL. Guidelines for accurate EC50/IC50 estimation. *Pharm Stat.* March 2011. Vol. 10(2). P: 128–34.
- 36- Fishmann TO, Hruza A, Duca JS, Ramanathan L, Mayhood T, Windsor WT, et al. Structure-guided discovery of cyclin-dependent kinase inhibitors. *Biopolymers.* May 2008. Vol. 89(5). P: 372–9.
- 37- Jevtovic V, Alshammari N, Latif S, Alsukaibi AKD, Humaidi J, Alanazi TYA, et al. Synthesis, Crystal Structure, Theoretical Calculations, Antibacterial Activity, Electrochemical Behavior, and Molecular Docking of Ni(II) and Cu(II) Complexes with Pyridoxal-Semicarbazone. *Molecules.* October 2022. Vol. 27(19).
- 38- Shang ZH, Sun JN, Guo JS, Sun YY, Weng WZ, Zhang ZX, et al. Facile synthesis of 1,3,4-oxadiazoles via iodine promoted oxidative annulation of methyl-azaheteroarenes and hydrazides. *Tetrahedron.* February 2020. Vol. 76(6).

